

# Josephson effect for SU(4) carbon-nanotube quantum dots

A. Zazunov,<sup>1</sup> A. Levy Yeyati,<sup>2</sup> and R. Egger<sup>1</sup>

<sup>1</sup>*Institut für Theoretische Physik, Heinrich-Heine-Universität, D-40225 Düsseldorf, Germany*

<sup>2</sup>*Departamento de Física Teórica de la Materia Condensada C-V, Universidad Autónoma de Madrid, E-28049 Madrid, Spain*

(Received 24 November 2009; published 8 January 2010)

We present the theory of the Josephson effect in nanotube dots where an SU(4) symmetry can be realized. We find a remarkably rich phase diagram that significantly differs from the SU(2) case. In particular,  $\pi$ -junction behavior is largely suppressed. We analytically obtain the Josephson current in various parameter regions: (i) in the Kondo regime covering the full crossover from SU(4) to SU(2), (ii) for weak tunnel couplings, and (iii) for a large BCS gap. The transition between these regions is studied numerically.

DOI: [10.1103/PhysRevB.81.012502](https://doi.org/10.1103/PhysRevB.81.012502)

PACS number(s): 74.50.+r, 73.63.-b, 74.78.Na

## I. INTRODUCTION

Several experimental groups have recently started to study the Josephson effect in ultrasmall nanostructures,<sup>1</sup> where the supercurrent can be tuned via the gate voltage dependence of the electronic levels of the nanostructure. An important system class where supercurrents have been successfully observed<sup>2</sup> is provided by carbon-nanotube (CNT) quantum dots. In many cases, the experimental results compare quite well to predictions based on modeling the CNT dot as a spin-degenerate electronic level with SU(2) spin symmetry, where the presence of a repulsive on-dot charging energy  $U$  may allow for a (normal-state) Kondo effect. Depending on the ratio  $T_K/\Delta$ , where  $\Delta$  is the energy gap in the superconducting electrodes and  $T_K$  the Kondo temperature, theory<sup>3-8</sup> predicts a transition between a unitary (maximum) Josephson current for  $\Delta \ll T_K$ , possible thanks to the survival of the Kondo resonance in that limit, and a  $\pi$ -junction regime for  $\Delta \gg T_K$ , where the critical current is small and negative, i.e., the junction free-energy  $F(\varphi)$  has a minimum at phase difference  $\varphi = \pi$  as opposed to the more common 0-junction behavior.

Recent progress has paved the way for the fabrication of very clean CNTs, resulting in a generation of quantum transport experiments and thereby revealing interesting physics, e.g., spin-orbit coupling effects<sup>9</sup> or incipient Wigner crystal behavior.<sup>10</sup> In ultraclean CNTs, the orbital degree of freedom ( $\alpha = \pm$ ) reflecting clockwise and anticlockwise motion around the CNT circumference (i.e., the two  $K$  points) is approximately conserved when electrons enter or leave the dot.<sup>11</sup> Due to the combined presence of this orbital “pseudospin” (denoted in the following by  $T$ ) and the true electronic spin ( $S$ ), an enlarged SU(4) symmetry group can be realized. In addition, a purely orbital SU(2) symmetry arises when a Zeeman field is applied. Experimental support for this scenario has already been published<sup>12</sup> (for the case of semiconductor dots, see Ref. 13) and several aspects have been addressed theoretically.<sup>11,14</sup> In particular, the SU(4) Kondo regime is characterized by an enhanced Kondo temperature and exotic local Fermi liquid behavior, where the Kondo resonance is asymmetric with respect to the Fermi level. However, so far both experiment and theory have only studied the case of normal conducting leads, where conventional linear response transport measurements cannot reliably

distinguish the SU(4) from the SU(2) scenario.<sup>14</sup> Here we provide the first theoretical study of the Josephson effect for interacting quantum dots with (approximate) SU(4) symmetry, and find drastic differences compared to the standard SU(2) picture. In the Kondo limit, a qualitatively different current-phase relation (CPR) is found, with the critical current smaller by a factor  $\approx 0.59$ . The usual  $\pi$ -junction behavior is largely suppressed, but unconventional phases do appear and time-reversal symmetry can be spontaneously broken. Our predictions can be tested using state-of-the-art experimental setups, and offer clear signatures of the SU(4) symmetry in very clean CNT quantum dots.

## II. MODEL AND FORMAL SOLUTION

We study a quantum dot ( $H_d$ ) contacted via a standard tunneling Hamiltonian ( $H_t$ ) to two identical superconducting electrodes ( $H_{L/R}$ ),  $H = H_d + H_t + H_L + H_R$ . We assume that the dot has a spin- and orbital-degenerate electronic level  $\epsilon_{\alpha\sigma} = \epsilon$  with identical intra- and inter-orbital charging energy  $U$ ,<sup>15</sup>  $H_d = \epsilon \hat{n} + U \hat{n}(\hat{n} - 1)/2$  with  $\hat{n} = \sum_{\alpha\sigma} d_{\alpha\sigma}^\dagger d_{\alpha\sigma}$ , where  $d_{\alpha\sigma}^\dagger$  creates a dot electron with spin  $\sigma = \uparrow, \downarrow = \pm$  and orbital pseudospin projection  $\alpha$ . Since the  $\alpha = \pm$  states are related by time-reversal symmetry (clockwise and anticlockwise states are exchanged), we take the lead Hamiltonian as

$$H_j = \sum_{k\alpha\sigma} \xi_k c_{jk\alpha\sigma}^\dagger c_{jk\alpha\sigma} + \sum_{k\alpha} (\Delta e^{\mp i(\varphi/2)} c_{jk\alpha\uparrow}^\dagger c_{j,-k,-\alpha,\downarrow} + \text{H.c.}),$$

where  $c_{jk\alpha\sigma}^\dagger$  creates an electron with wave vector  $k$  in lead  $j = L/R$ , and  $\xi_k$  is the single-particle energy. The tunneling Hamiltonian is  $H_t = \sum_{jk\sigma,\alpha\alpha'} (t \delta_{\alpha\alpha'} + \tilde{t} \delta_{\alpha,-\alpha'}) c_{jk\alpha\sigma}^\dagger d_{\alpha'\sigma} + \text{H.c.}$ , where  $t$  ( $\tilde{t}$ ) describes orbital (non)conserving tunneling processes. Following standard steps,<sup>4</sup> the noninteracting lead fermions can now be integrated out. The partition function  $Z(\varphi) = e^{-\beta F(\varphi)}$  at inverse temperature  $\beta$  then reads (we often set  $e = \hbar = 1$ )

$$Z(\varphi) = \text{Tr}_d (e^{-\beta H_d} \mathcal{T} e^{-\int_0^\beta d\tau d\tau' D^\dagger(\tau) \Sigma(\tau-\tau') D(\tau')}), \quad (1)$$

where the trace extends over the dot Hilbert space,  $\mathcal{T}$  denotes time ordering, and we use the Nambu bispinor  $D = (d_{e\uparrow}, d_{e\downarrow}, d_{o\uparrow}, d_{o\downarrow})$  with even/odd linear combinations of the orbital states,  $d_{e\sigma} = (d_{+\sigma} + d_{-\sigma})/\sqrt{2}$  and  $d_{o\sigma} = \sigma(d_{+\sigma} - d_{-\sigma})/\sqrt{2}$ . In this basis, the self-energy  $\Sigma(\tau)$  representing

the BCS leads is diagonal in orbital space. With the orbital mixing angle  $\theta=2 \tan^{-1}(\tilde{t}/t)$  and the normal-state density of states  $\nu_0=2\sum_k\delta(\xi_k)$ , the even/odd channels are characterized by the hybridization widths  $\Gamma_{\nu=e,o}=(1\pm\sin\theta)\Gamma$  with  $\Gamma=\pi\nu_0(t^2+\tilde{t}^2)$ . In what follows, we study the zero-temperature limit and assume the wide-band limit<sup>1</sup> for the leads. The Fourier transformed self-energy is then expressed in terms of the  $2\times 2$  Nambu matrices

$$\Sigma_{\nu=e,o}(\omega)=\frac{\Gamma_{\nu}}{\sqrt{\omega^2+\Delta^2}}\begin{pmatrix} -i\omega & \Delta\cos\frac{\varphi}{2} \\ \Delta\cos\frac{\varphi}{2} & -i\omega \end{pmatrix}.$$

The result (1) will now be examined in several limits. We start with the strong-correlation limit  $U\rightarrow\infty$ , and later address the case of finite  $U$ . Note that Eq. (1) for  $\theta=0$  corresponds to the SU(4) symmetric case while for  $\theta=\pi/2$  there is only one conducting channel with nonzero transmission which, under certain conditions, corresponds to the usual SU(2) model.

### III. DEEP KONDO LIMIT

Let us first discuss the Kondo limit  $T_K\gg\Delta$  in the quarter-filled case,  $\epsilon<0$  and  $\langle\hat{n}\rangle\approx 1$ . The Kondo temperature is given by  $T_K=D\exp(\pi\epsilon/4\Gamma)$ <sup>11</sup> with bandwidth  $D$ . As in the SU(2) case,<sup>3</sup> the Josephson current at  $T=0$  can be computed from local Fermi-liquid theory, either using phase shift arguments or an equivalent mean-field slave-boson treatment.<sup>5</sup> The latter approach yields the self-consistent dot level  $\tilde{\epsilon}$  and thereby the transmission probability for channel  $\nu=e,o$ ,<sup>11</sup>

$$T_{\nu}=\frac{(1\pm\sin\theta)^2T_K^2}{\tilde{\epsilon}^2+(1\pm\sin\theta)^2T_K^2}, \quad \frac{\tilde{\epsilon}}{T_K}=\frac{(1-\sin\theta)^{(\sin\theta+1)/4}}{(1+\sin\theta)^{(\sin\theta-1)/4}}. \quad (2)$$

In the SU(4) case ( $\theta=0$ ), we have  $T_e=T_o=1/2$ , while the SU(2) limit ( $\theta=\pi/2$ ) has a decoupled odd channel,  $T_e=1$  and  $T_o=0$ . The CPR covering the crossover from the SU(4) to the SU(2) Kondo regime then follows as

$$I(\varphi)=\frac{e\Delta}{2\hbar}\sum_{\nu=e,o}\frac{T_{\nu}\sin\varphi}{\sqrt{1-T_{\nu}\sin^2\frac{\varphi}{2}}}. \quad (3)$$

The known SU(2) result<sup>3</sup> is recovered for  $\theta=\pi/2$ . The SU(4) CPR has a completely different shape, as shown in Fig. 1. We note that the critical current  $I_c=\max[I(\varphi)]$  is suppressed by the factor  $2-\sqrt{2}\approx 0.59$  relative to the unitary limit  $e\Delta/\hbar$  reached for the SU(2) dot. The Josephson current in the deep Kondo regime is thus very sensitive to the SU(4) vs SU(2) symmetry.

### IV. PERTURBATION THEORY IN $\Gamma$

Next we address the opposite limit of very small  $\Gamma\ll\Delta$ , where lowest-order perturbation theory in  $\Gamma$  applies. After some algebra, Eq. (1) for  $\theta=0$  yields the CPR of a tunnel

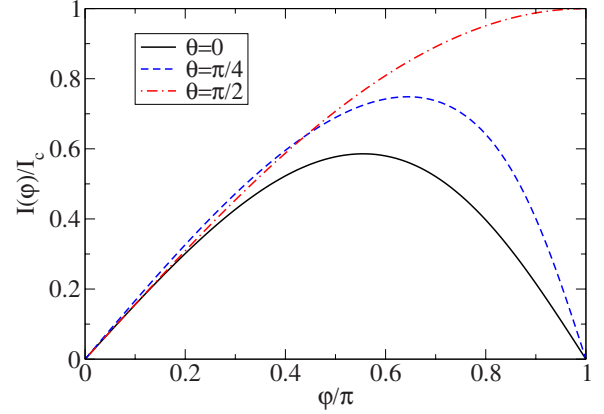


FIG. 1. (Color online) Josephson CPR in the Kondo limit for various  $\theta$ . The SU(4) case corresponds to  $\theta=0$ , the SU(2) case to  $\theta=\pi/2$ . The supercurrent is given in units of the unitary limit  $I_c=e\Delta/\hbar$ .

junction,  $I(\varphi)=I_c\sin(\varphi)$ , where the critical current is

$$I_c=[4\Theta(\epsilon)-\Theta(-\epsilon)]F(|\epsilon|/\Delta)I_0, \quad (4)$$

with the Heaviside function  $\Theta$ , the current scale  $I_0=\Delta(\Gamma/\pi\Delta)^2$ , and (see also Ref. 16)

$$F(x)=\frac{(\pi/2)^2(1-x)-\arccos^2x}{2x(1-x^2)}.$$

In this  $U\rightarrow\infty$  limit, the dot contains one electron for (finite)  $\epsilon<0$ , and thus we have spin  $S=1/2$ . Equation (4) shows that such a magnetic junction displays a  $\pi$  phase. For the SU(4) case, the ratio  $I_c(-|\epsilon|)/I_c(|\epsilon|)=-1/4$  is twice smaller than in the SU(2) case, i.e.,  $\pi$ -junction behavior tends to be suppressed. This tendency is also confirmed for  $U\ll\Delta$  (see below), where the  $\pi$  phase is in fact essentially absent. The factor 1/4 can be understood in simple terms by counting the number of possible processes leading to a Cooper pair transfer through the dot.<sup>17,18</sup> When  $\epsilon>0$ , there are four possibilities corresponding to the quantum numbers  $(\alpha,\sigma)$  of the first electron entering the dot. However, for  $\epsilon<0$  there is only one possibility since an electron already occupies the dot and then only one specific choice of  $(\alpha,\sigma)$  allows for Cooper pair tunneling. This argument is readily generalized to the SU(2N) case, where the above ratio of critical currents is obtained as  $-1/2N$ .

### V. EFFECTIVE HAMILTONIAN FOR $\Delta\rightarrow\infty$

The partition function (1) simplifies considerably when  $\Delta$  exceeds all other energy scales of interest. Then the dynamics is always confined to the subgap region (Andreev states) and quasiparticle tunneling processes from the leads (continuum states) are negligible. In particular, this allows to study the case  $U\ll\Delta$ . In fact, for  $\Delta\rightarrow\infty$ , with the Cooper pair operators  $b_1^\dagger=d_{e_1}^\dagger d_{o_1}^\dagger$  and  $b_2^\dagger=d_{o_1}^\dagger d_{e_1}^\dagger$ , Eq. (1) is equivalently described by the effective dot Hamiltonian

$$H_\infty=H_d+\cos(\varphi/2)[\Gamma_e b_1+\Gamma_o b_2+\text{H.c.}]. \quad (5)$$

The resulting Hilbert space can be decomposed into three decoupled sectors<sup>19</sup> according to spin  $S$  and orbital pseu-

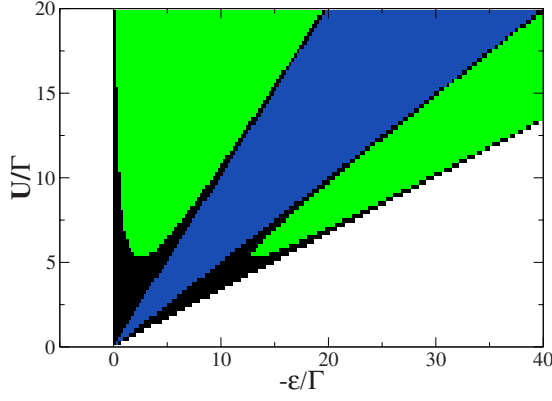


FIG. 2. (Color online) Phase diagram for  $\Delta \rightarrow \infty$ . White regions correspond to  $(S, T)=0$ , and green regions to  $(S, T)=1/2$ . In the black regions, the ground state has  $(S, T)=0$  for  $\varphi=0$  and  $(S, T)=1/2$  for  $\varphi=\pi$ . For the blue region, we have  $(S, T)=0$  at  $\varphi=0$  and  $(S, T)=1$  at  $\varphi=\pi$ . (Ref. 20)

dospin  $T$  (notice that these quantities are localized on the dot for  $\Delta \rightarrow \infty$ ). The ground-state energy  $E_g(\varphi) = \min(E_{(S,T)})$  then determines the Josephson current  $I(\varphi) = 2\partial_\varphi E_g(\varphi)$ . (i) The  $(S, T)=0$  sector is spanned by the four states  $\{|0\rangle, b_1^\dagger|0\rangle, b_2^\dagger|0\rangle, b_1^\dagger b_2^\dagger|0\rangle\}$ , where  $|0\rangle$  is the empty dot state. The matrix representation reads

$$H_{(S,T)=0} = \begin{pmatrix} 0 & \Gamma_e \cos \frac{\varphi}{2} & \Gamma_o \cos \frac{\varphi}{2} & 0 \\ \Gamma_e \cos \frac{\varphi}{2} & E_2 & 0 & \Gamma_o \cos \frac{\varphi}{2} \\ \Gamma_o \cos \frac{\varphi}{2} & 0 & E_2 & \Gamma_e \cos \frac{\varphi}{2} \\ 0 & \Gamma_o \cos \frac{\varphi}{2} & \Gamma_e \cos \frac{\varphi}{2} & E_4 \end{pmatrix},$$

with the eigenenergies  $E_n = \epsilon n + Un(n-1)/2$  of the decoupled dot. The lowest energy  $E_{(S,T)=0} = E_2 + z$  then follows from the smallest root of the quartic equation  $\Pi_\pm[z^2 - 2zU - (\Gamma_e \pm \Gamma_o)^2 \cos^2 \frac{\varphi}{2}] = (E_4 z / 2)^2$ . (ii) The  $(S, T)=1/2$  sector can be decomposed into four subspaces with one or three electrons according to  $S_z = \pm 1/2$  and Cooper pair channel  $\nu = e, o$ . The Hamiltonian is

$$H_{(S,T)=1/2}^{(\nu)} = \begin{pmatrix} E_1 & \Gamma_\nu \cos \frac{\varphi}{2} \\ \Gamma_\nu \cos \frac{\varphi}{2} & E_3 \end{pmatrix},$$

where  $H_{(S,T)=1/2}^{(e)}$  operates in the subspace spanned by  $\{d_{o1}^\dagger|0\rangle, b_1^\dagger d_{o1}^\dagger|0\rangle\}$  for  $S_z = +1/2$ , and  $\{d_{e1}^\dagger|0\rangle, b_1^\dagger d_{e1}^\dagger|0\rangle\}$  for  $S_z = -1/2$ . (Similarly, the subspaces corresponding to  $H_{(S,T)=1/2}^{(o)}$  are obtained by letting  $d_{\nu\sigma}^\dagger \rightarrow d_{\nu,-\sigma}^\dagger$  and  $b_1^\dagger \rightarrow b_2^\dagger$ .) With  $\Gamma_e \geq \Gamma_o$ , the lowest energy is  $E_{(S,T)=1/2} = (E_1 + E_3 - [(E_3 - E_1)^2 + 4\Gamma_e^2 \cos^2(\varphi/2)]^{1/2})/2$ . (iii) Finally, the  $(S, T)=(1, 0)$  sector is spanned by the two uncoupled two-particle states  $d_{e,\sigma}^\dagger d_{o,\sigma}^\dagger|0\rangle$ , with  $\varphi$ -independent energy  $E_{S=1, T=0} = E_2$ . In addition, there are two decoupled  $(S, T)=(0, 1)$  states  $d_{\nu 1}^\dagger d_{\nu 1}^\dagger|0\rangle$  with the same energy  $E_2$ . In the limit  $\Delta \rightarrow \infty$ , this  $(S, T)=1$  sector is energetically unfavorable except possibly at  $\varphi=\pi$ .

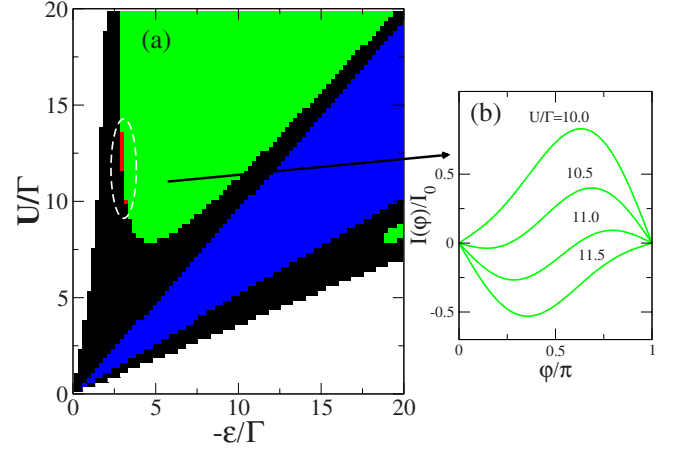


FIG. 3. (Color online) (a) Same as Fig. 2 but for  $\Delta=10\Gamma$  within the zero-bandwidth limit for the leads (see text). Although the  $\Delta \rightarrow \infty$  phase diagram is basically reproduced, for finite  $\Delta$ , the  $(S, T)=1/2$  phase (green) exhibits a crossover from 0- to  $\pi$ -junction behavior for  $U \approx \Delta$ , as illustrated in panel (b), where the CPR is shown for  $\epsilon/\Gamma = -5$  and several  $U$ ; the current is normalized to  $I_0$ , see Eq. (4). Moreover, a phase with  $(S, T)=0$  at  $\varphi=0$  and  $(S, T)=1/2$  at  $\varphi=\pi$  appears, where (contrary to the “black” phase)  $\varphi=\pi$  corresponds to the lowest energy ( $\pi'$  behavior), indicated in red [within the dashed ellipses in panel (a)].

## VI. PHASE DIAGRAM FOR $\Delta \gg \Gamma$

Next we discuss the resulting phase diagram in the  $SU(4)$  limit ( $\theta=0$ ). The result for  $\Delta \rightarrow \infty$  is shown in Fig. 2 in the  $U-\epsilon$  plane. The phases are classified according to the three sectors defined above.<sup>20</sup> The reported phases are specific for the  $SU(4)$  symmetry and are qualitatively different from the standard  $SU(2)$  case. We observe that the  $\varphi$ -dependence of the  $\Delta \rightarrow \infty$  ground-state energy implies 0-junction behavior for both  $S=0$  and  $S=1/2$ . While the magnetic  $S=1/2$  sector often represents a  $\pi$ -junction,<sup>3,4,6</sup> in multilevel dots there is no direct connection between the spin and the sign of the Josephson coupling.<sup>18</sup> The  $\pi$ -phase found under perturbation theory [Eq. (4) for  $\epsilon < 0$ ] is in fact restricted to the regime  $U \gg \Delta$ , while for  $U \ll \Delta$ , the  $S=1/2$  state displays a 0-phase. In the intermediate regime one should therefore observe a crossover between those two behaviors. Interestingly, there are parameter regions with a spin/pseudospin transition as  $\varphi$  varies. For instance, the “black” regions in Fig. 2 correspond to a mixed state with  $(S, T)=0$  at  $\varphi=0$  and  $(S, T)=1/2$  at  $\varphi=\pi$ , while for the “blue” region, the ground state is in the  $(S, T)=0$  sector except at  $\varphi=\pi$  where it crosses to the  $(S, T)=1$  sector.

We find that these phases are also observable at finite  $\Delta \geq \Gamma$ , where we have employed two complementary approaches. First, a full numerical solution is possible when approximating each electrode by a single site (zero-bandwidth limit), which can provide a satisfactory, albeit not quantitative, understanding of the phase diagram.<sup>8</sup> Second, one can go beyond the above  $\Delta \rightarrow \infty$  limit by including cotunneling processes in a systematic way. Both approaches give essentially the same results, and here we only show results from the single-site model. As can be observed in Fig.

3(a), the overall features of the  $\Delta \rightarrow \infty$  phase diagram are reproduced for finite  $\Delta$ , with somewhat shifted boundaries between the different regions. In particular, in the “green” ( $S=1/2$ ) regime, this calculation captures the mentioned transition from a 0-junction at  $\Delta \gg U$  to a  $\pi$  junction at  $\Delta \ll U$ , as illustrated in Fig. 3(b). Consequently, for finite  $\Delta$ , the “black” phase may now have lowest energy at  $\varphi=\pi$ , implying the  $\pi'$  phase<sup>4,6,8</sup> indicated in “red” in Fig. 3(a). Finally, for the junctions with  $U/\Gamma=10.5$  and 11 in Fig. 3(b), the ground state is realized at phase difference  $0 < \varphi < \pi$ , which implies that time-reversal symmetry is spontaneously broken here.

To conclude, we have studied the Josephson current in SU(4) symmetric quantum dots, including the crossover to the standard SU(2) symmetric case. Contrary to normal-state transport, the supercurrent is very sensitive to the symmetry group and should allow to observe clear signatures of the

SU(4) state in ultraclean CNT dots. In particular, the  $\pi$  phase is largely suppressed, the CPR in the Kondo limit has a distinctly different shape and a smaller critical current, and the phase diagram turns out to be quite rich. In addition, following Ref. 21, we expect a strongly reduced thermal noise in the deep SU(4) Kondo regime since [in contrast to the SU(2) case] there are two channels with imperfect transmission. Future theoretical work is needed to give a quantitative understanding of the crossover between the various regimes discussed above.

#### ACKNOWLEDGMENTS

This work was supported by the SFB TR/12 of the DFG, the EU network HYSWITCH, the ESF network INSTANS, and by the Spanish MICINN under Contracts No. FIS2005-06255 and No. FIS2008-04209.

<sup>1</sup>Yu. V. Nazarov and Ya. M. Blanter, *Quantum transport: Introduction to nanoscience* (Cambridge University Press, Cambridge, 2009).

<sup>2</sup>A. Y. Kasumov *et al.*, *Science* **284**, 1508 (1999); A. F. Morpurgo *et al.*, *ibid.* **286**, 263 (1999); M. R. Buitelaar, T. Nussbaumer, and C. Schönberger, *Phys. Rev. Lett.* **89**, 256801 (2002); P. Jarillo-Herrero, J. A. van Dam, and L. P. Kouwenhoven, *Nature (London)* **439**, 953 (2006); J.-P. Cleuziou *et al.*, *Nat. Nanotechnol.* **1**, 53 (2006); H. I. Jorgensen, K. Grove-Rasmussen, T. Novotny, K. Flensberg, and P. E. Lindelof, *Phys. Rev. Lett.* **96**, 207003 (2006); A. Eichler, R. Deblock, M. Weiss, C. Karrasch, V. Meden, C. Schönberger, and H. Bouchiat, *Phys. Rev. B* **79**, 161407(R) (2009).

<sup>3</sup>L. I. Glazman and K. A. Matveev, *JETP Lett.* **49**, 659 (1989).

<sup>4</sup>A. V. Rozhkov and D. P. Arovas, *Phys. Rev. Lett.* **82**, 2788 (1999).

<sup>5</sup>A. A. Clerk and V. Ambegaokar, *Phys. Rev. B* **61**, 9109 (2000); A. V. Rozhkov and D. P. Arovas, *ibid.* **62**, 6687 (2000).

<sup>6</sup>F. Siano and R. Egger, *Phys. Rev. Lett.* **93**, 047002 (2004); M. S. Choi, M. Lee, K. Kang, and W. Belzig, *Phys. Rev. B* **70**, 020502(R) (2004); G. Sellier, T. Kopp, J. Kroha, and Y. S. Barash, *ibid.* **72**, 174502 (2005); C. Karrasch, A. Oguri, and V. Meden, *ibid.* **77**, 024517 (2008); M. Governale, M. G. Pala, and J. König, *ibid.* **77**, 134513 (2008).

<sup>7</sup>A. Zazunov, A. Schulz, and R. Egger, *Phys. Rev. Lett.* **102**, 047002 (2009); T. Meng, S. Florens, and P. Simon, *Phys. Rev. B* **79**, 224521 (2009).

<sup>8</sup>E. Vecino, A. Martín-Rodero, and A. Levy Yeyati, *Phys. Rev. B* **68**, 035105 (2003).

<sup>9</sup>F. Kuemmeth *et al.*, *Nature (London)* **452**, 448 (2008).

<sup>10</sup>V. V. Deshpande and M. Bockrath, *Nat. Phys.* **4**, 314 (2008); V. V. Deshpande *et al.*, *Science* **323**, 106 (2009).

<sup>11</sup>J. S. Lim, M. S. Choi, M. Y. Choi, R. Lopez, and R. Aguado, *Phys. Rev. B* **74**, 205119 (2006).

<sup>12</sup>P. Jarillo-Herrero *et al.*, *Nature (London)* **434**, 484 (2005); A.

Makarovski, A. Zhukov, J. Liu, and G. Finkelstein, *Phys. Rev. B* **75**, 241407(R) (2007); A. Makarovski, J. Liu, and G. Finkelstein, *Phys. Rev. Lett.* **99**, 066801 (2007); T. Delattre *et al.*, *Nat. Phys.* **5**, 208 (2009).

<sup>13</sup>S. Sasaki, S. Amaha, N. Asakawa, M. Eto, and S. Tarucha, *Phys. Rev. Lett.* **93**, 017205 (2004).

<sup>14</sup>L. Borda, G. Zarand, W. Hofstetter, B. I. Halperin, and J. von Delft, *Phys. Rev. Lett.* **90**, 026602 (2003); M. S. Choi, R. López, and R. Aguado, *ibid.* **95**, 067204 (2005); K. Le Hur, P. Simon, and D. Loss, *Phys. Rev. B* **75**, 035332 (2007); C. A. Büsser and G. B. Martins, *ibid.* **75**, 045406 (2007); C. Mora, X. Leyronas, and N. Regnault, *Phys. Rev. Lett.* **100**, 036604 (2008); P. Vitushinsky, A. A. Clerk, and K. Le Hur, *ibid.* **100**, 036603 (2008); F. B. Anders, D. E. Logan, M. R. Galpin, and G. Finkelstein, *ibid.* **100**, 086809 (2008).

<sup>15</sup>It is straightforward to allow for orbital or Zeeman fields or for more general interactions. We also consider identical tunnel couplings between the dot and both electrodes. Asymmetries produce similar effects as the orbital mixing  $\tilde{t}$  in  $H_r$ .<sup>11</sup>

<sup>16</sup>T. Novotný, A. Rossini, and K. Flensberg, *Phys. Rev. B* **72**, 224502 (2005).

<sup>17</sup>B. I. Spivak and S. A. Kivelson, *Phys. Rev. B* **43**, 3740 (1991).

<sup>18</sup>Y. Shimizu, H. Horii, Y. Takane, and Y. Isawa, *J. Phys. Soc. Jpn.* **67**, 1525 (1998); A. V. Rozhkov, D. P. Arovas, and F. Guinea, *Phys. Rev. B* **64**, 233301 (2001).

<sup>19</sup>Different phases can be labeled by  $S^2+T^2$ , and we use the notation  $(S,T)=0$  for  $S=T=0$ ,  $(S,T)=1/2$  for  $S=T=1/2$ , and  $(S,T)=1$  for both  $(S,T)=(1,0)$  and  $(0,1)$ .

<sup>20</sup>Strictly speaking, precisely at  $\Delta=\infty$  there are degeneracies that make the classification ambiguous. However, at finite  $\Delta$ , Fig. 3 indicates that the reported phases are stable. We have also confirmed their stability for  $\theta \neq 0$ .

<sup>21</sup>A. Martín-Rodero, A. Levy Yeyati, and F. J. García-Vidal, *Phys. Rev. B* **53**, R8891 (1996).